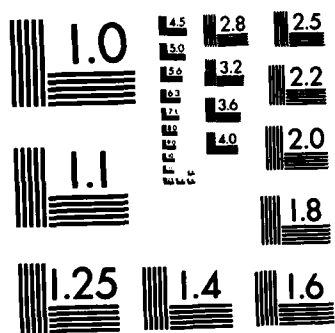


AD-A123 322 MESOPHASE BEHAVIOR IN CARBON FIBER BUNDLES(U) AEROSPACE 1/1  
CORP EL SEGUNDO CA MATERIALS SCIENCES LAB  
J L WHITE ET AL. 01 JUN 82 TR-0082(2728-01)-1  
UNCLASSIFIED SD-TR-82-88 F04701-81-C-0082 F/G 11/4 NL





MICROCOPY RESOLUTION TEST CHART  
NATIONAL BUREAU OF STANDARDS-1963-A

(12)

ADA123322

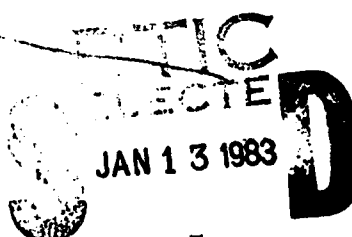
## Mesophase Behavior in Carbon Fiber Bundles

J. L. WHITE, C. B. NG,  
P. M. SHEAFFER, and M. BUECHLER  
Materials Sciences Laboratory  
Laboratory Operations  
The Aerospace Corporation  
El Segundo, Calif. 90245

1 June 1982

APPROVED FOR PUBLIC RELEASE;  
DISTRIBUTION UNLIMITED

Prepared for  
**OFFICE OF NAVAL RESEARCH**  
Washington, D.C. 22217  
**SPACE DIVISION**  
**AIR FORCE SYSTEMS COMMAND**  
Los Angeles Air Force Station  
P.O. Box 92960, Worldway Postal Center  
Los Angeles, Calif. 90009



1 COPY

03 01 13 011

This report was submitted by The Aerospace Corporation, El Segundo, CA 90245, under Contract No. F04701-81-C-0082 with the Space Division, Deputy for Technology, P.O. Box 92960, Worldway Postal Center, Los Angeles, CA 90009. It was reviewed and approved for The Aerospace Corporation by L. R. McCreight, Director, Materials Sciences Laboratory. 2nd Lt Steven G. Hancock, SD/YLXS, was the project officer for Technology.

This report has been reviewed by the Public Affairs Office (PAS) and is releasable to the National Technical Information Service (NTIS). At NTIS, it will be available to the general public, including foreign nations.

This technical report has been reviewed and is approved for publication. Publication of this report does not constitute Air Force approval of the report's findings or conclusions. It is published only for the exchange and stimulation of ideas.

Steven G. Hancock

Steven G. Hancock, 2nd Lt, USAF  
Project Officer

David T. Newell

David T. Newell, Lt Colonel, USAF  
Acting Director, Space Systems Technology

FOR THE COMMANDER

Norman W. Lee

Norman W. Lee, Jr., Colonel, USAF  
Commander, Det 1, AFSTC

**UNCLASSIFIED**

**SECURITY CLASSIFICATION OF THIS PAGE (When Data Entered)**

DD FORM 1473  
(FACSIMILE)

**UNCLASSIFIED**

**SECURITY CLASSIFICATION OF THIS PAGE (When Data Entered)**

UNCLASSIFIED

SECURITY CLASSIFICATION OF THIS PAGE(When Data Entered)  
19. KEY WORDS (Continued)

20. ABSTRACT (Continued)

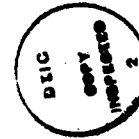
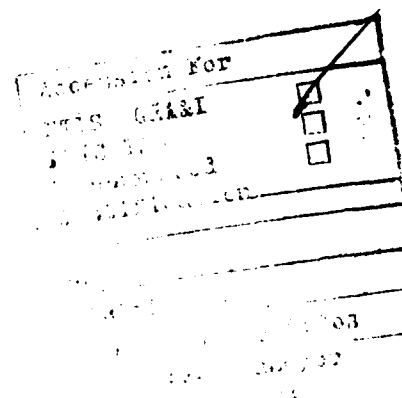
within the open wedge of radially structured fiber. After pyrolysis through the stage of mesophase hardening, the matrix porosity appears to depend on the constraint of the fiber bundle. The mesophase at that stage is a fragile solid easily fractured by local stresses within the fiber bundle.

A

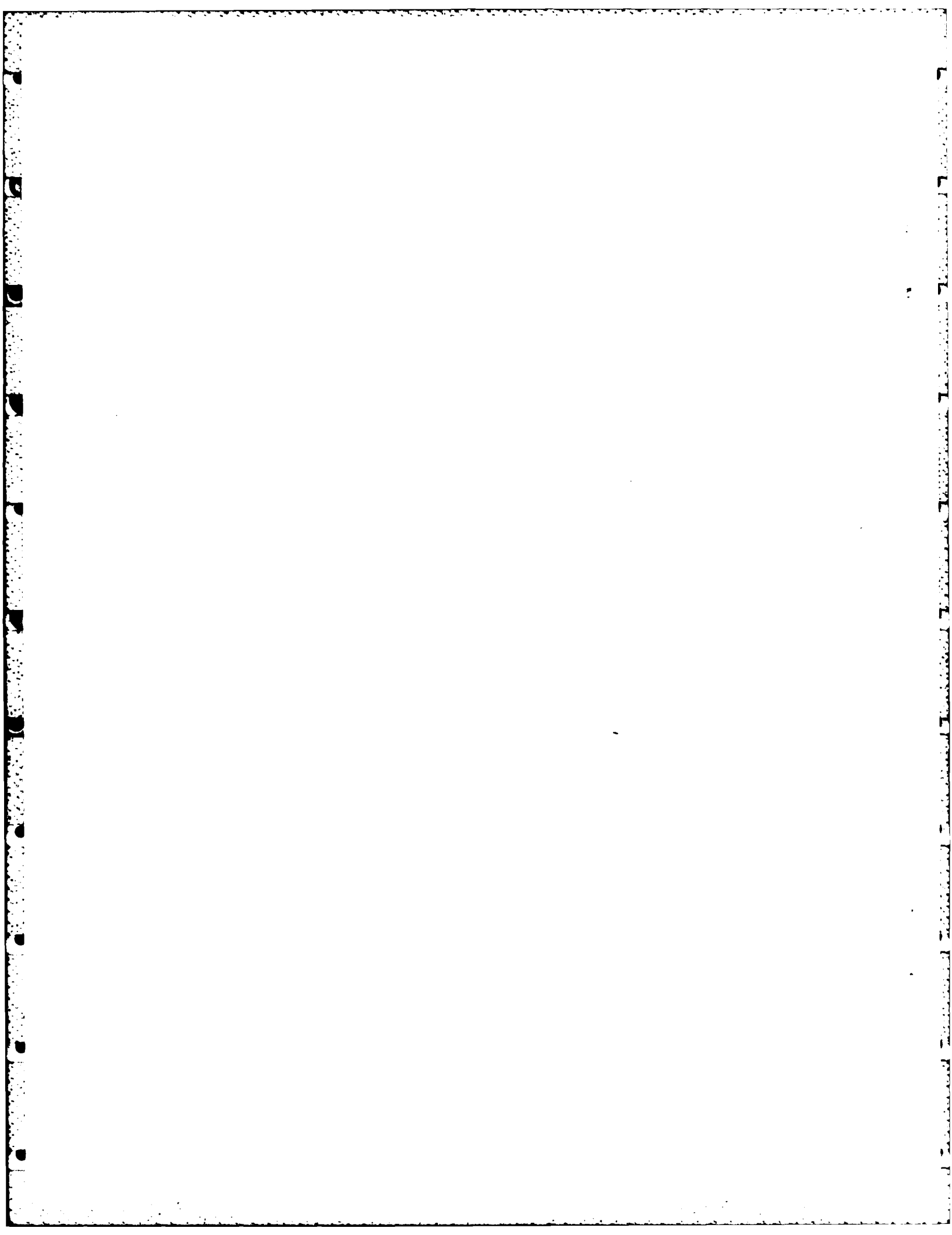
UNCLASSIFIED  
SECURITY CLASSIFICATION OF THIS PAGE(When Data Entered)

## CONTENTS

I.	INTRODUCTION.....	5
II.	EXPERIMENTAL.....	7
	A. IN-AUTOCLAVE QUENCHING.....	7
	B. FIBER-BUNDLE HOLDER.....	8
	C. MICROGRAPHIC PREPARATION.....	11
III.	MICROGRAPHIC OBSERVATIONS.....	13
	A. PYROLYSIS TO 430°C.....	13
	B. PYROLYSIS TO 505°C.....	16
IV.	DISCUSSION.....	25
	REFERENCES.....	27



A



## FIGURES

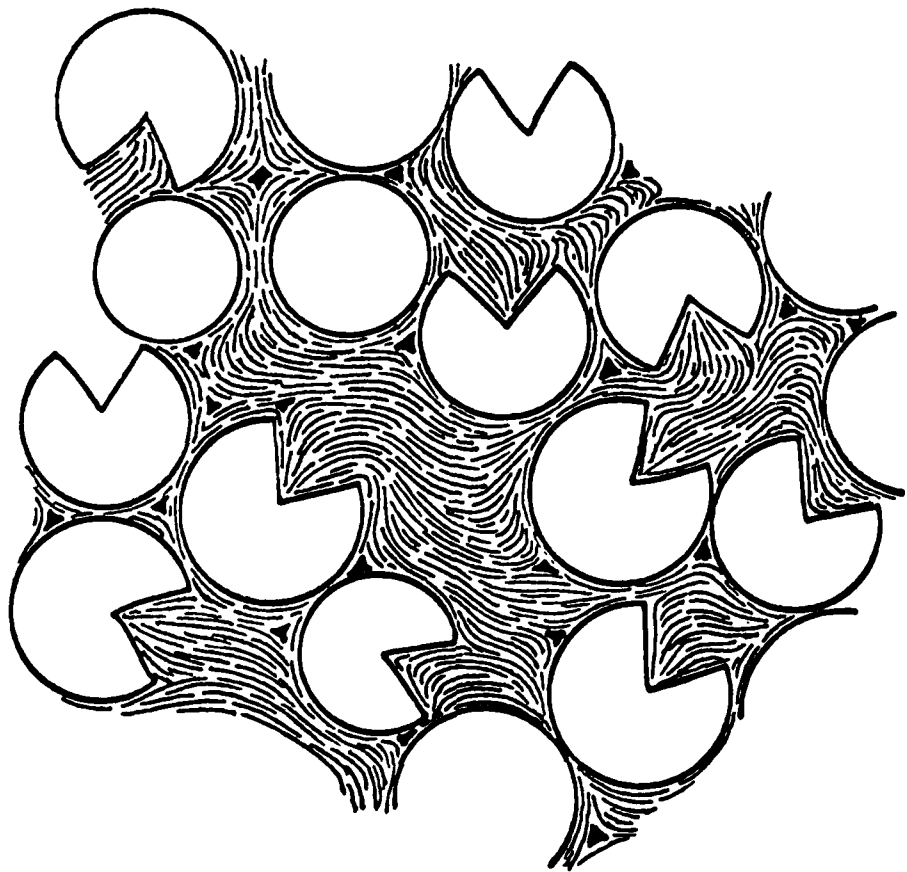
1. Sheath Effect Observed Within Bundle of Mesophase Carbon Fibers.....	6
2. Fiber-Bundle Holder.....	9
3. Structural Models of Mesophase Carbon Fiber.....	10
4. Constrained and Open Fiber Bundles at 430°C Pyrolysis Condition.....	14
5. Constrained and Open Fiber Bundles at 430°C Pyrolysis Condition.....	15
6. Open Fiber Bundle at 430°C Pyrolysis Condition.....	17
7. Coarse Mesophase Formed Under Quiescent Conditions.....	18
8. Mesophase Wetting of Unrestrained Fibers.....	19
9. Constrained and Open Fiber Bundles at 505°C Pyrolysis Condition.....	20
10. Constrained and Open Fiber Bundles at 505°C Pyrolysis Condition.....	21
11. Mesophase Wetting and Fracture at Pores in Open Fiber Bundle; 505°C Pyrolysis Condition.....	23

## I. INTRODUCTION

The high-temperature properties of carbon-fiber-reinforced carbon-matrix composites have established them as leading candidate materials for many structural applications that demand resistance to thermal shock, strength at temperature, and resistance to erosion by hot high-velocity gas streams. Such composites are fabricated by processes in which a pregraphitic matrix is formed by impregnating a three-dimensional woven-fiber preform with coal-tar or petroleum pitches that pass through a mesophase (liquid-crystal) state upon carbonization.<sup>1</sup> Thus the carbonaceous mesophase may be expected to play a key role in fabrication by determining the morphology of the composite matrix, as well as the number of impregnation and graphitization cycles required to achieve the desired levels of composite density.

Figure 1 illustrates the matrix morphology developed within a fiber bundle by a single impregnation of a woven preform for a specimen that has been pyrolyzed to hardened mesophase. The tendency for the mesophase layers to align with the substrate surface (usually described as the "sheath effect") dominates the matrix morphology and determines its disclination structures.<sup>2</sup> Although knowledge of the steps by which this morphology develops is clearly fundamental to an understanding of composite processing, the experimental difficulty of obtaining specimens quenched at high pressure and representative of stages in which the mesophase is fluid has effectively deterred such studies.

We have found the method of interrupted pyrolysis to be effective in studying the formation of mesophase microstructures in petroleum coking.<sup>3</sup> Therefore, in the present work, we apply similar techniques to the high-pressure processing of carbon-carbon composites. This report briefly describes some preliminary experiments in room-pressure pyrolysis undertaken to test our experimental approach. It is published at this time because the micrographic observations on specimens pyrolyzed at room pressure confirm and carry forward some significant observations recently reported by Cranmer et al.<sup>4</sup>



▼ - $\pi$  WEDGE DISCLINATION

★ - $2\pi$  WEDGE DISCLINATION

Fig. 1. Sheath Effect Observed Within Bundle of Mesophase Carbon Fibers. Lamelliform morphology of mesophase layers, indicated by dashed lines, has been mapped out by response to polarized light, using an immersion oil to enhance contrast.<sup>2</sup> Filled symbols locate positions of negative wedge disclinations.

## II. EXPERIMENTAL

The preliminary work addressed three problems of experimental technique:

1. An in-autoclave quenching technique to freeze the mesophase morphology while maintaining the specimen under pressure.
2. The design and test of a simple fixture to hold fiber bundles under conditions approximating those of composite fabrication.
3. The micrographic preparation of composite specimens in which soft, freshly precipitated mesophase is in direct contact with relatively hard carbon fibers.

### A. IN-AUTOCLOVE QUENCHING

A reasonable quenching rate must be achieved for specimens containing partially transformed mesophase so that the liquid-crystalline structures existing at the point of quench are frozen in place.<sup>5</sup> It is impractical to quench the mass of a hot-wall autoclave, and explosive hazards can arise if a coolant is introduced directly onto a specimen within the high-pressure hot zone. However, previous experience in studies of mesophase formation in petroleum coking<sup>3</sup> suggested that the self-cooling of a low-thermal-inertia furnace within a cold-wall autoclave might provide an adequate quench. Rapid cooling is required only in the initial stages; hot-stage observations<sup>6</sup> indicate that most mesophase specimens are frozen solid by 250°C.

Accordingly, a simple furnace with only electrical insulation was fitted into the 2-in. internal diameter of the autoclave at our disposal. The power required to attain mesophase-forming temperatures (400-550°C), as well as the cooling rates on power switch-off, were observed. The results were favorable: for example, in one run in air at room pressure, 450°C was attained at a power of 120 W, switch-off gave an initial cooling rate of 67°C/min, and 250°C was arrived at in 3.8 min. Thus the method of self-cooling within a cold-wall autoclave appears satisfactory, and a furnace designed specifically for the autoclave is now being constructed to provide uniform heating to an aluminum pyrolysis cell of the type used in previous studies.<sup>7</sup>

### B. FIBER-BUNDLE HOLDER

An aluminum fixture was designed to fit within the pyrolysis cell and to hold the fiber bundles under three conditions: (1) restrained within a well-defined cavity, (2) open to penetration from the side by the impregnant pitch, and (3) open at the splayed end to penetration from the end as well as the side. The fixture, depicted in Fig. 2, provides channels for four different fibers to be pyrolyzed under identical conditions. Only four micrographic sections are required to observe open, constrained, and splayed fiber bundles in both longitudinal and transverse sections.

The practicability of this design was tested in a room-pressure pyrolysis furnace that permits a number of pyrolysis cells to be subjected to identical thermal programs.<sup>7</sup> Some fixtures were positioned with vertical fibers to determine whether orientation affects results. The pyrolysis schedule was 20°C/hr to 360°C and 5°C/hr to the desired quench temperature, at which time the selected cell was withdrawn and cooled by being inserted into a cold copper block. The impregnant was Ashland A240 petroleum pitch in amounts sufficient to completely cover the bundle holder upon melt-down. As defined by the withdrawal temperature, two pyrolysis states were studied: 430°C, at which point the mesophase transformation is well under way; and 505°C, at which point mesophase hardening should be complete but shrinkage only just begun. Carbon fiber spun from mesophase pitch was selected for the room-pressure pyrolyses to permit comparison with recently reported work.<sup>4</sup> Three basic morphologies of mesophase carbon fibers are illustrated by Fig. 3.<sup>8</sup> The fiber lot selected for the pyrolysis tests was composed primarily of radial filaments with graphite layer-faces exposed in the open wedge; however, some round fibers with random or oriented cores were also present.

After pyrolysis and quenching, the fiber-bundle holders were recovered by cleaning away sufficient pyrolysis residue to identify the geometry of the bundle holders. For support, each specimen was then encapsulated in epoxy resin so that longitudinal and transverse sections could be cut, as indicated by planes A through D in Fig. 2. A diamond wire saw was used for the cutting.

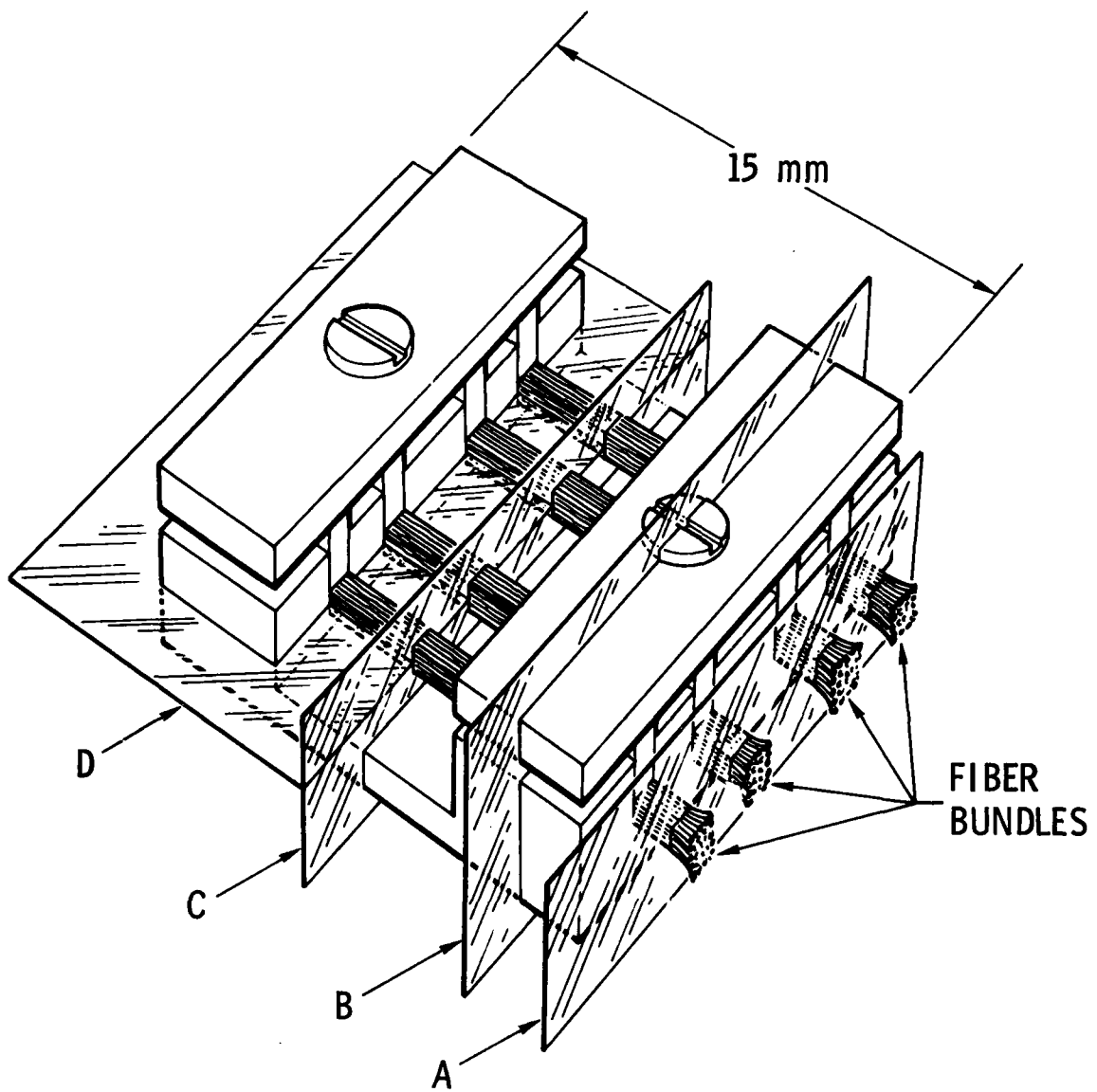


Fig. 2. Fiber-Bundle Holder. Aluminum fixture is designed to hold four fiber bundles under well-defined conditions of restraint during pyrolysis within a pool of impregnant pitch. Planes A, B, and C define transverse sections for splayed, constrained, and open bundles, respectively; Plane D defines longitudinal sections for four fibers.

$\Delta = -\pi$  WEDGE DISCLINATION  
 $\bullet = +2\pi$  WEDGE DISCLINATION

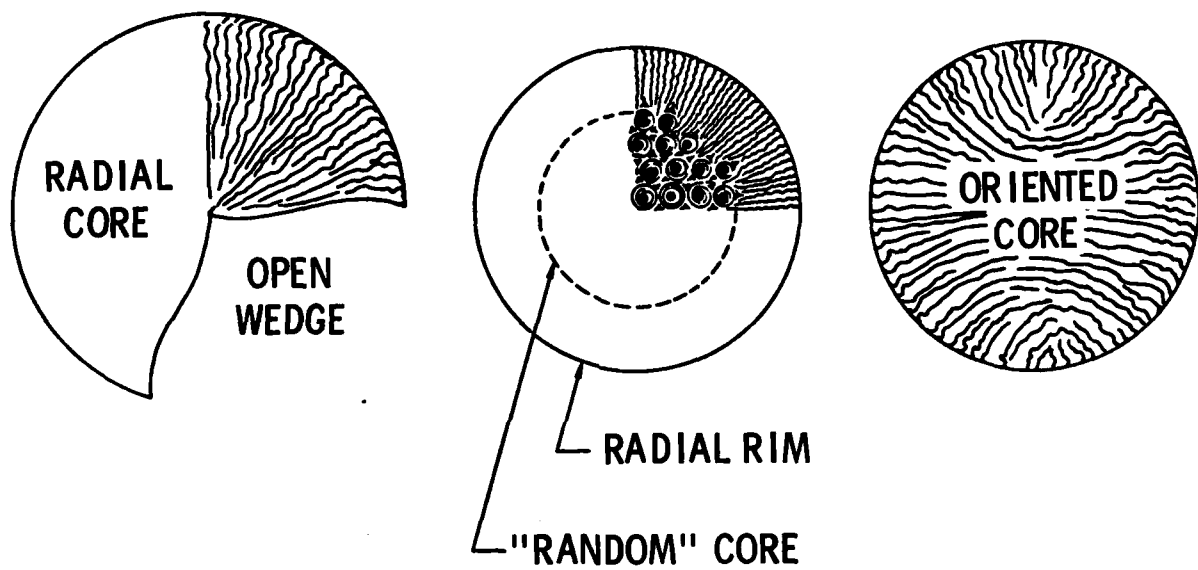


Fig. 3. Structural Models of Mesophase Carbon Fiber. Lines represent orientation of carbon layers.

C. MICROGRAPHIC PREPARATION

The techniques of micrographic preparation are critical in achieving an acceptably flat, polished surface on the partially pyrolyzed specimens. Drastic fine-scale variations in hardness and toughness of pitch, mesophase, fiber, and epoxy can pose problems of polishing relief that often tend to obscure the salient interface details that are of central interest in this study.

Reasonable success in minimizing relief, particularly in transverse specimens, has been achieved by wet polishing on bonded-grit papers down to a grit size of 0.3  $\mu\text{m}$ . Specimens were final polished in two steps: (1) with a polishing cloth to which cerium oxide had been applied and (2) by applying a thick, cerium oxide slurry, using the fingertip (protected by a rubber finger cot) as a sensitive lap. A mild detergent solution was used as the lubricant for all operations beyond 600-mesh grinding.

The transverse micrographs of Figs. 4 through 11 were photographed on specimens prepared by this two-step procedure. Polishing of longitudinal surfaces proved less successful, probably because of the elongated, closed porosity described in Section IV.

### III. MICROGRAPHIC OBSERVATIONS

The design of the fiber-bundle fixture proved satisfactory both for pyrolysis and for micrographic preparation. The position of a fixture within a coke lump was readily established with precision sufficient to cut the desired micrographic sections. No significant differences in microstructure were observed between fixtures oriented vertically and horizontally.

#### A. PYROLYSIS TO 430°C

The microstructures observed in specimens pyrolyzed to 430°C are presented in Figs. 4 through 8. Previous studies<sup>3</sup> of the pyrolysis of A240 petroleum pitch indicate that, under the pyrolysis conditions used here, the mesophase transformation should proceed to about 20 vol% if it is not affected by the presence of the fibrous substrate.

General views of transverse sections of constrained and open fiber bundles are compared in Fig. 4. The extensive formation of bulk mesophase around the open bundle is striking, displaying deformed microstructures apparently produced by bubble percolation or convective flow. The formation of the deformed bulk mesophase is consistent with hot-stage observations of the effects of flow on mesophase coalescence: Rester and Rowe<sup>9</sup> reported that coalescence was enhanced along paths of bubble percolation, and Cranmer et al.<sup>4</sup> observed mesophase coalescence and buildup in the wake of pyrolyzing pitch flowing over fibers or other obstacles.

Higher-magnification views within the fiber bundles are compared in Fig. 5. Mesophase fibers, the mesophase matrix, untransformed pitch, and gas pores can be distinguished by their characteristic responses to polarized light. The mesophase transformation within the fiber bundles has just begun. At this point, no significant differences appear between the constrained and open fiber bundles.

The individual filaments are wetted by both pitch and mesophase; careful examination of well-defined junctures of the mesophase-pitch interface with the fiber substrate revealed a slight, apparent preference to wetting by the pitch phase. Mesophase is often present within the open wedge of the radially

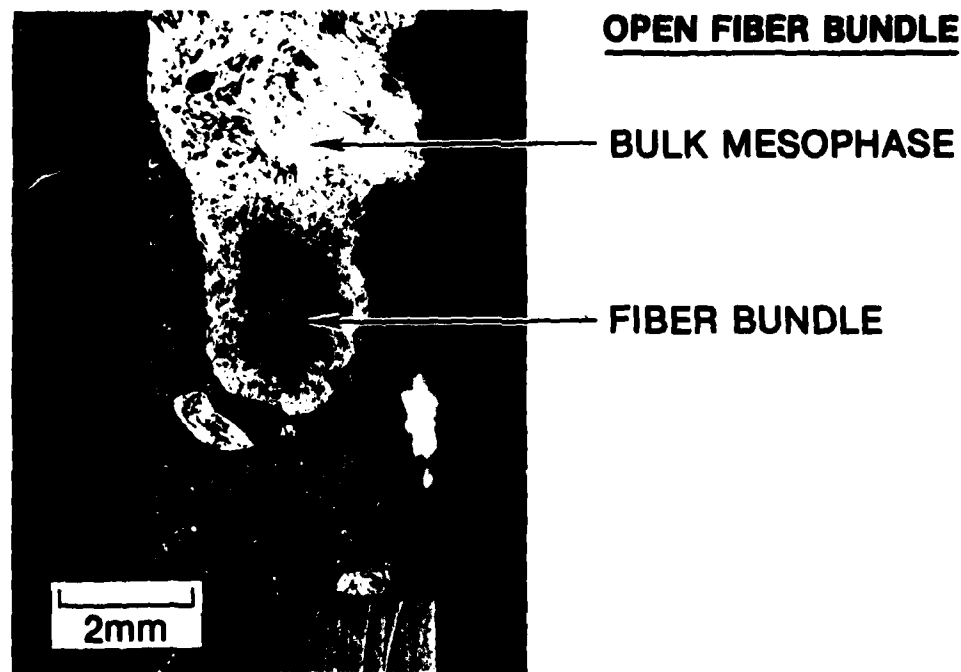
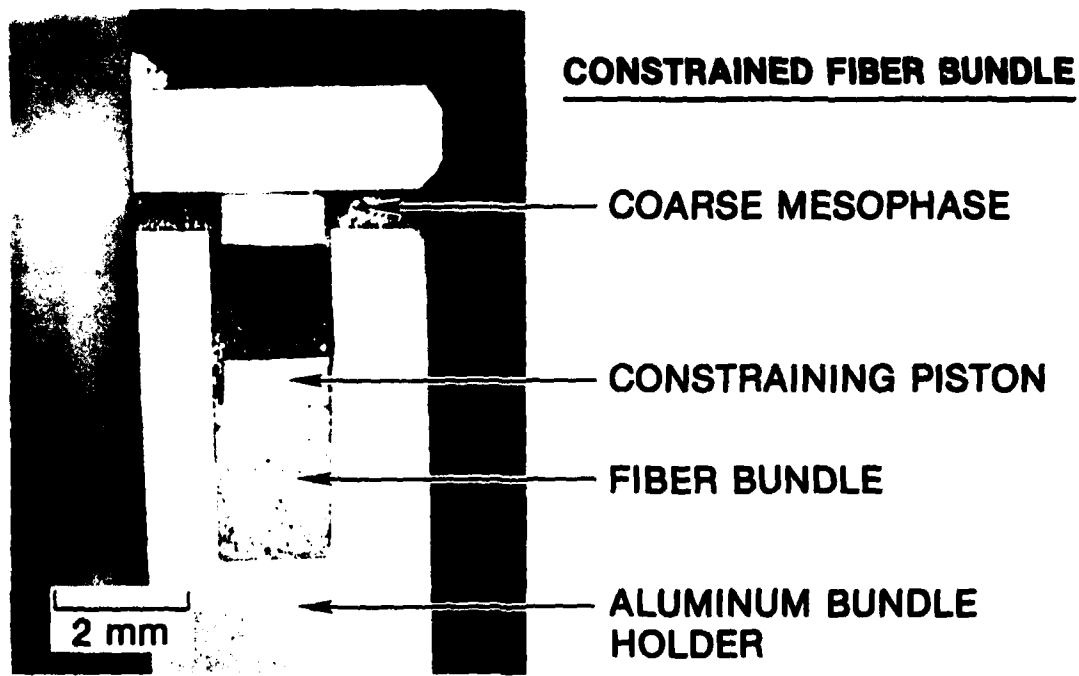


Fig. 4. Constrained and Open Fiber Bundles at 430°C Pyrolysis Condition.  
Transverse sections at low magnification. Crossed polarizers.

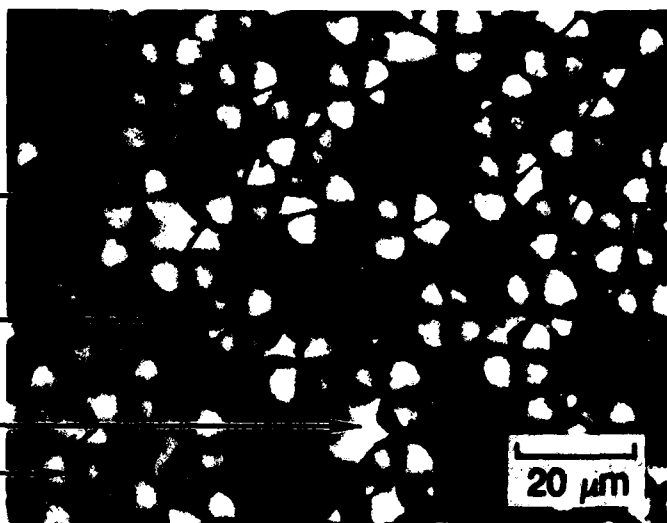
**CONSTRAINED**  
**FIBER BUNDLE**

PORE

PITCH

MESOPHASE

FILAMENT



**OPEN**  
**FIBER BUNDLE**

MESOPHASE

FILAMENT

PITCH

PORE

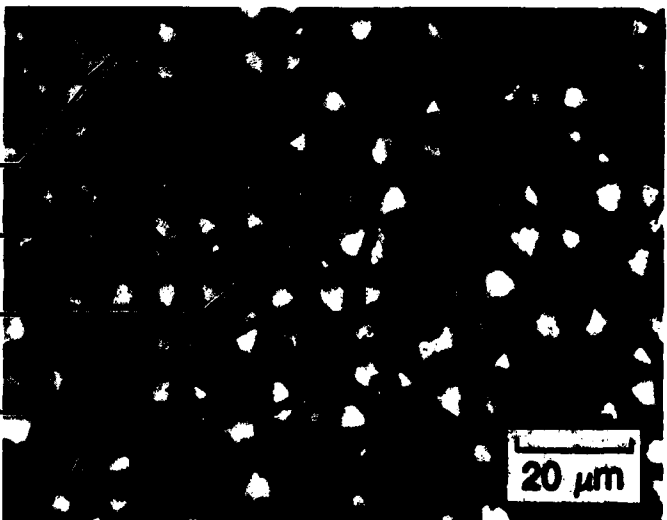


**Fig. 5.** Constrained and Open Fiber Bundles at 430°C Pyrolysis Condition.  
Regions near center of fiber bundles. Crossed polarizers.

structured filaments, and essentially all mesophase occurring within the bundles is in contact with fiber. Observations of mesophase alignment on the substrate surfaces confirmed the sheathlike orientations illustrated in Fig. 1: The mesophase layers lie parallel to the surface, whether it be the radial open wedge, the periphery of the open-wedge fiber, or the periphery of a round fiber.

The edge of the open bundle is illustrated by Fig. 6. A rim 100 to 200  $\mu\text{m}$  in depth is well impregnated by fully transformed mesophase. Within this region, the filaments appear more densely packed.

A mesophase body formed in a quiescent region of the restraining fixture is depicted in Fig. 7 to illustrate how coarsely structured the mesophase can grow when free of constraining surfaces and deformation. The wide spacing of polarized-light extinction contours corresponds to very gentle curvatures in the preferred orientation of the mesophase molecules and contrasts strongly with the layer curvatures required to conform with the geometrical constraints within a fiber bundle.

Some filaments that escaped from the constraining piston (see Fig. 8) demonstrate exceptions to the tendency for the mesophase to wet preferentially the open wedge of the radially structured filaments.

#### B. PYROLYSIS TO 505°C

Photomicrographs of fiber bundles in the condition of pyrolysis to 505°C, Figs. 9 through 11, demonstrate that the mesophase transformation has been completed. The mesophase is believed to be effectively solid at this quench temperature.

The low-magnification views of Fig. 9 indicate a significant difference in the nature of the porosity. The open bundle develops a coarser, more randomized porosity than does the constrained bundle. These differences are detailed in the higher magnification views in Fig. 10, in which the pores of the open bundle appear to have agglomerated, probably by local motions of the filaments, to produce larger pores separated by well-impregnated regions. The presence of some fractures in the mesophase matrix indicates that the mesophase had solidified at the quench temperature of 505°C.

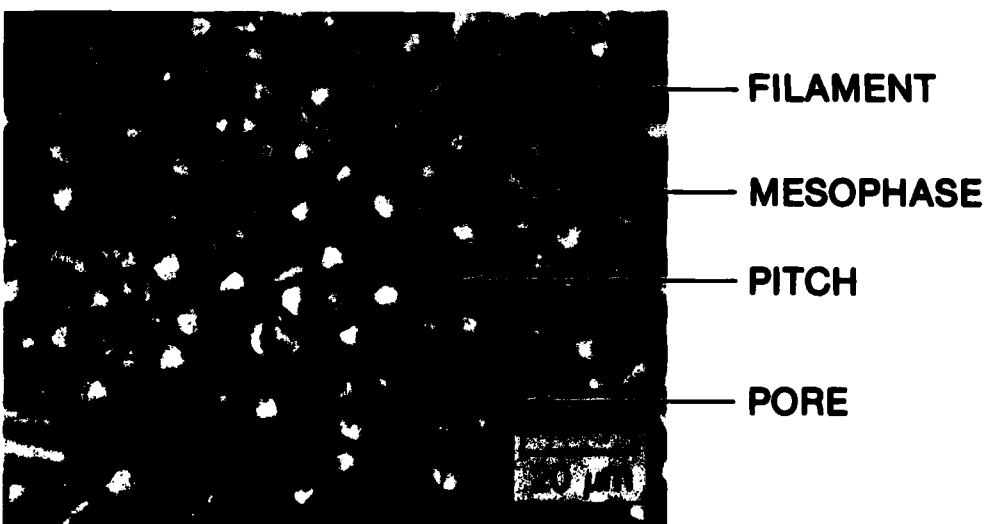
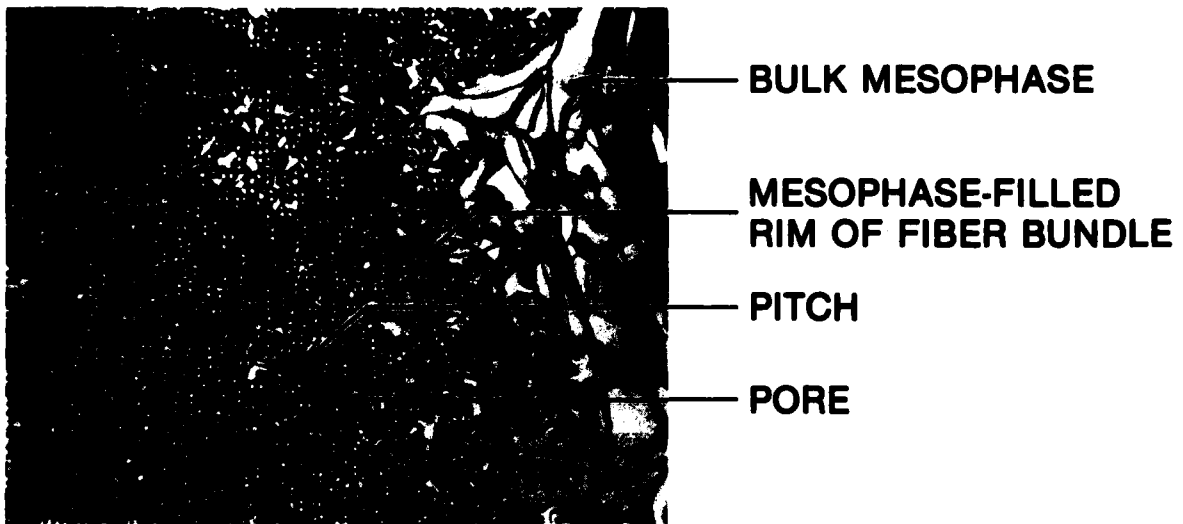
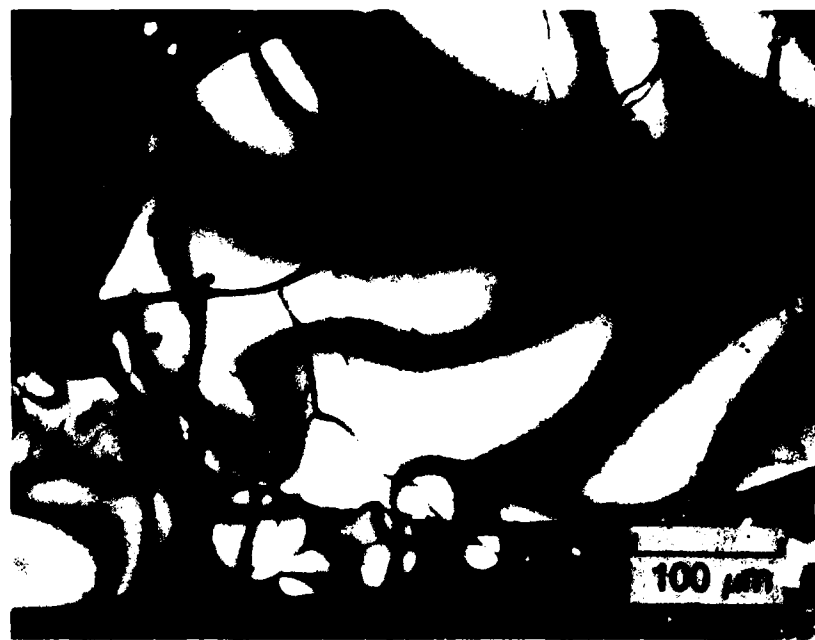
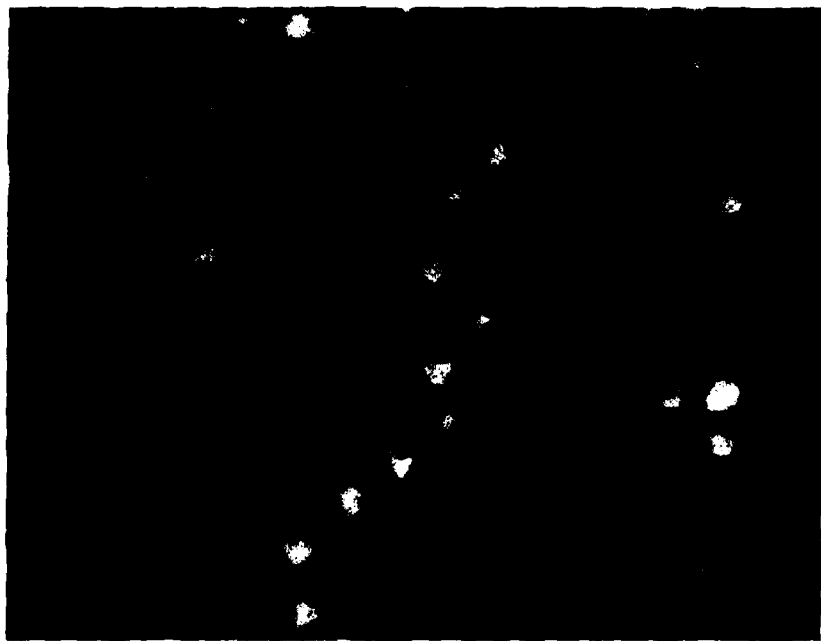


Fig. 6. Open Fiber Bundle at 430°C Pyrolysis Condition. Region at edge of fiber bundle. Crossed polarizers.



**Fig. 7.** Coarse Mesophase Formed Under Quiescent Conditions. Pyrolysis condition, 430°C. From Fig. 4, upper view. Crossed polarizers.



**Fig. 8.** Mesophase Wetting of Unrestrained Fibers. Pyrolysis condition,  
430°C. Crossed polarizers.

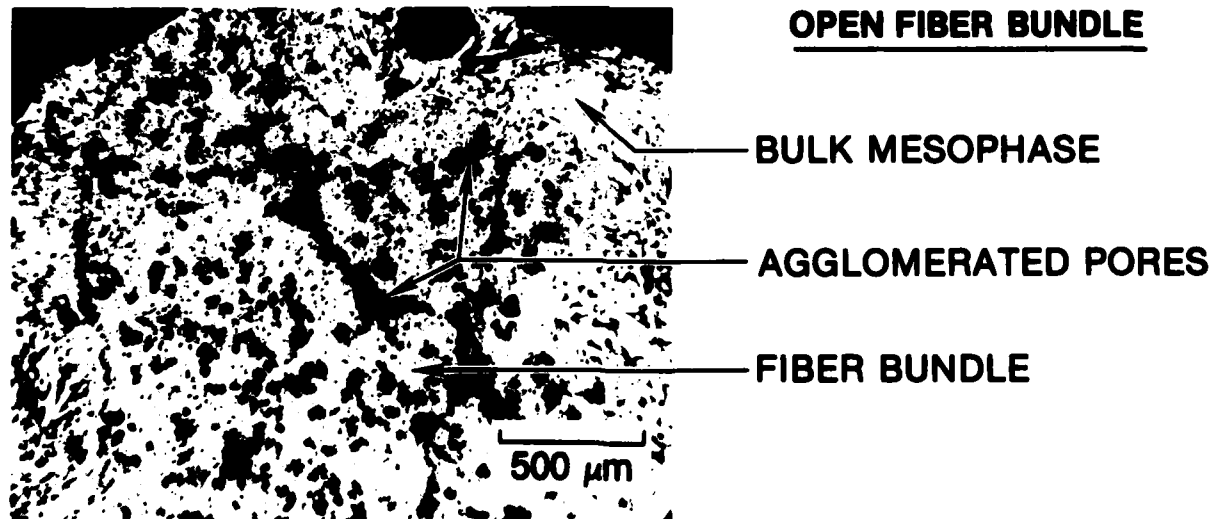
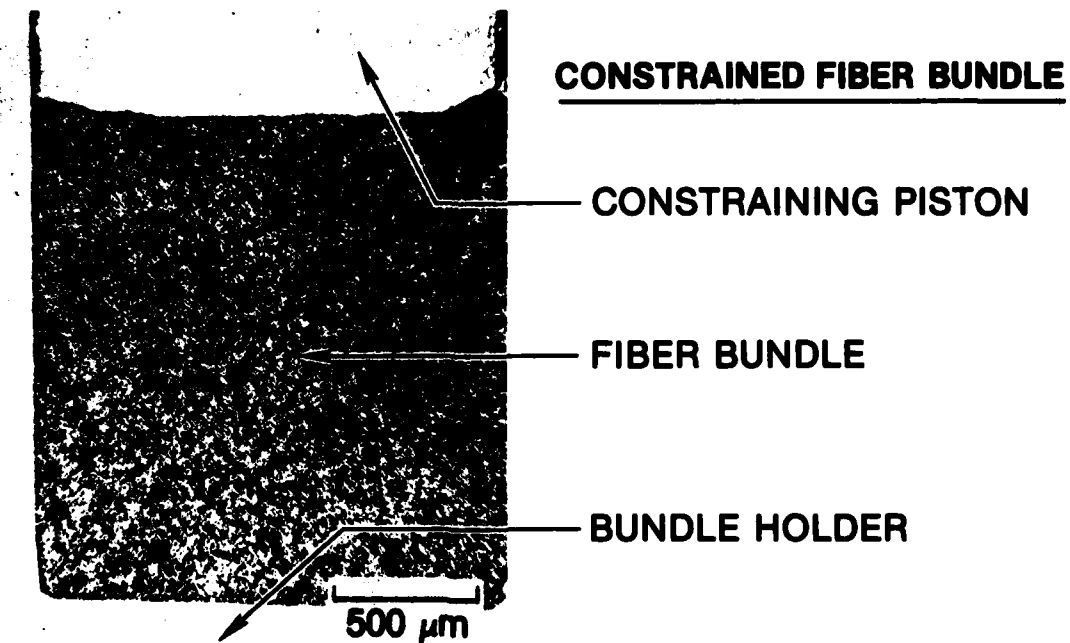
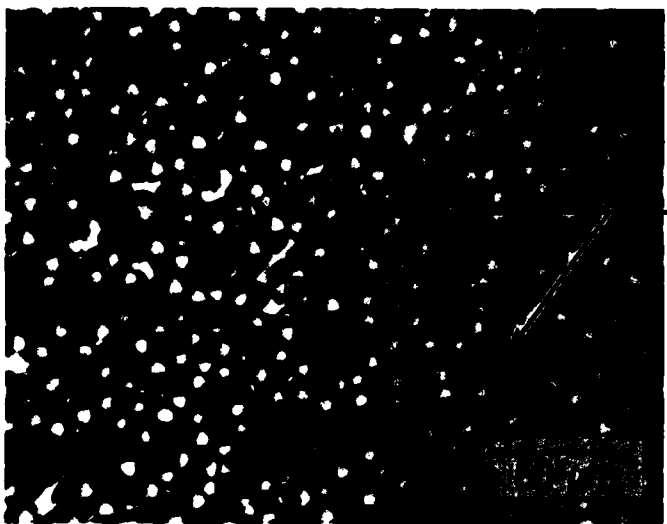
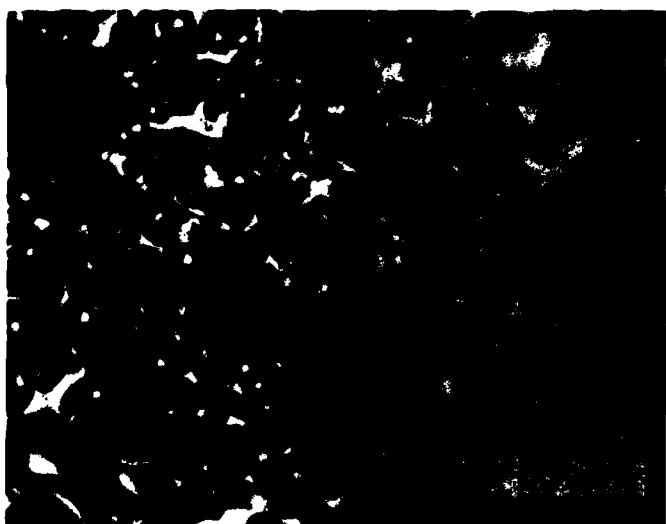


Fig. 9. Constrained and Open Fiber Bundles at 505°C Pyrolysis Condition.  
Transverse sections at low magnification. Crossed polarizers.



**CONSTRINED  
FIBER BUNDLE**

— PORES



**OPEN  
FIBER BUNDLE**

— FRACTURE

— AGGLOMERATED  
PORE

**Fig. 10. Constrained and Open Fiber Bundles at 505°C Pyrolysis Condition.  
Regions near center of fiber bundles. Crossed polarizers.**

The open fiber bundle is further magnified in Fig. 11, which was taken at the limit of optical resolution with an immersion oil. From the figure, it can be observed that, as the mesophase hardened, it formed a near-zero wetting angle on the fiber substrate, both on peripheral and open-wedge surfaces. The fine fractures visible throughout the matrix imply that, at this stage of pyrolysis, the mesophase is fragile and easily fractured by local stresses within a fiber bundle. No special preference for fracture is evidenced at the fiber-mesophase interface. Cleavage fracture parallel to the mesophase layers appears to be favored over fracture across such layers.

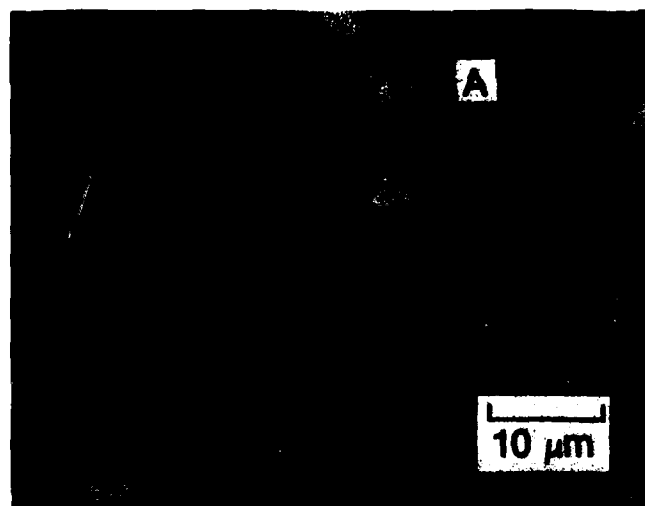
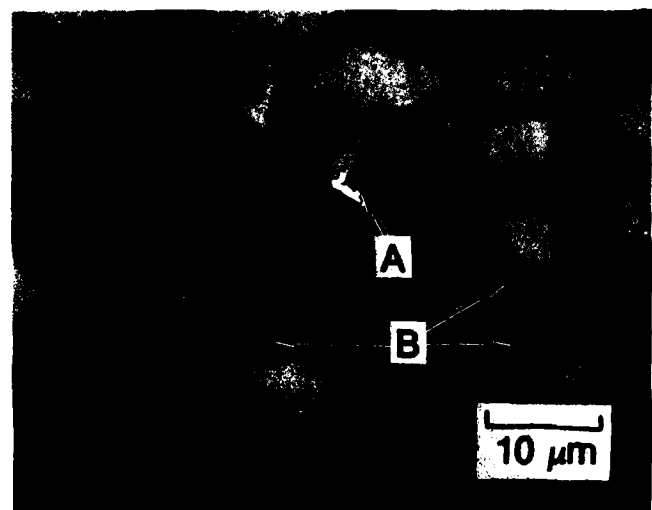


**Fig. 11. Mesophase Wetting and Fracture at Pores in Open Fiber Bundle; 505°C Pyrolysis Condition.** Near-zero wetting angles appear both on open-wedge surfaces (A) and on the periphery (B) of the mesophase fiber. Immersion oil, polarizer only.

#### IV. DISCUSSION

From our observations in this study, and with experience gained in pyrolyzing petroleum feedstocks,<sup>3</sup> we conclude that three stages of pyrolysis should be distinguished. This differentiation is useful because the mechanisms that form the matrix morphology are distinct in each stage, as are the micrographic polishing procedures required to permit observations near the limit of optical resolution.

In the first stage of pyrolysis, the pitch is the continuous phase of the matrix, at least within the fiber bundle on which our interest is centered. The mesophase transforms and coalesces more rapidly outside the bundle, which may be due to the flow effects noted by Cranmer et al.,<sup>4</sup> as well as to the lower susceptibility of the bundle interior to the loss of volatile species.<sup>10</sup> Within the fiber bundle, the filaments are wet by both mesophase and pitch, and the precipitating mesophase is almost always present on a fiber surface, with some apparent preference for the open-wedge segment of radially structured filaments. The relatively low porosity may be attributed to easier percolation of bubbles from a fluid pitch matrix and to the small amount of gas formed. At this stage, the micrographic observations are limited by the extent to which a flat surface can be achieved on the soft pitch and mesophase and by the tendency of these materials to dissolve in the immersion oils commonly used to increase the resolving power.

In the second stage of pyrolysis, the mesophase becomes the continuous phase, and the structural mechanisms appear to be bubble nucleation, pore agglomeration, and bloating to drive mesophase from the fiber bundle. Since the porosity is closed and elongated along the fibers, a satisfactory polish of a longitudinal section may require an additional specimen impregnation after the appropriate section has been opened by cutting and rough polishing to within about 20  $\mu\text{m}$  of the final polished surface.

The third stage of pyrolysis extends from the point of mesophase hardening to the final heat treatment that may be applied to carbon-carbon composites. This stage thus includes the phenomena of anisotropic shrinkage

and the opening of shrinkage cracks, which would be more evident at temperatures considerably higher than employed in the present study.<sup>1</sup> The fragility of the mesophase immediately after hardening, as inferred from Fig. 11, emphasizes the need for better knowledge of the mechanical properties, particularly in the 500-to-1000°C temperature range, in which the dimensional changes are most rapid.<sup>1</sup> The polishing techniques must be adjusted to accommodate the varying hardness of the coked and heat-treated mesophase.<sup>11</sup>

In addition to confirming that the mesophase transformation proceeds differently in a fiber bundle than in bulk pyrolysis and that the matrix morphology is dominated by the alignment of mesophase layers parallel to the substrate,<sup>2</sup> the present results direct attention to the role of wetting and bloating phenomena in determining the extent and nature of the matrix porosity. Mesophase bloating, a familiar problem at the large scale of petroleum coking,<sup>3</sup> also operates at the micrometer scale of fiber interstices to produce pores that can agglomerate to varying degrees depending on the freedom of movement of individual filaments. The extents to which these phenomena are affected by pressure and by fiber-bundle constraints will be focal points in the pyrolysis studies at high pressure.

## REFERENCES

1. J. L. White, "The Formation of Microstructure in Graphitizable Materials," Prog. Solid State Chem. 9, 55 (1975).
2. J. E. Zimmer and J. L. White, "Disclination Structures in the Carbonaceous Mesophase," Adv. Liq. Cryst. 5, in press.
3. J. L. White, "Mesophase Mechanisms in the Formation of Microstructure of Petroleum Coke," in Petroleum Derived Carbons, Am. Chem. Soc. Symp. Series, No. 21, eds. M. L. Deviney and T. M. O'Grady, 282 (1976).
4. J. H. Cranmer, I. G. Plotzker, L. H. Peebles, Jr., and D. R. Uhlmann, "Dynamic Interaction of Mesophase Spherules with Various Surfaces," Ext. Abstr., 15th Conf. Carbon, 180 (1981).
5. R. T. Lewis, "Hot-Stage Microscopy of Mesophase Pitches," Ext. Abstr., 12th Conf. Carbon, 215 (1975).
6. M. Buechler, C. B. Ng, and J. L. White, "Disclination Interactions in the Carbonaceous Mesophase," Ext. Abstr., 15th Conf. Carbon, 182 (1981).
7. V. L. Weinberg and J. L. White, Pitch Fractionation, TR-0082(2935-02)-1, The Aerospace Corporation, El Segundo, Calif. (15 December 1981).
8. J. L. White, C. B. Ng, M. Buechler, and E. J. Watts, "Microstructure of Mesophase Carbon Fiber," Ext. Abstr., 15th Conf. Carbon, 310 (1981).
9. D. O. Rester and C. R. Rowe, "Effect of Gas Bubble Formation and Percolation of the Carbonaceous Mesophase from Acenaphthylene," Carbon 12, 218 (1974).
10. D. M. Riggs and R. J. Diefendorf, "A Phase Diagram for Pitches," Carbon '80, 3rd International Carbon Conference, 326 (1980).
11. J. Dubois, C. Agace, and J. L. White, "The Carbonaceous Mesophase Formed in the Pyrolysis of Graphitizable Organic Materials," Metallography 3, 337 (1970).

#### LABORATORY OPERATIONS

The Laboratory Operations of The Aerospace Corporation is conducting experimental and theoretical investigations necessary for the evaluation and application of scientific advances to new military space systems. Versatility and flexibility have been developed to a high degree by the laboratory personnel in dealing with the many problems encountered in the nation's rapidly developing space systems. Expertise in the latest scientific developments is vital to the accomplishment of tasks related to these problems. The laboratories that contribute to this research are:

Aerophysics Laboratory: Launch vehicle and reentry aerodynamics and heat transfer, propulsion chemistry and fluid mechanics, structural mechanics, flight dynamics; high-temperature thermomechanics, gas kinetics and radiation; research in environmental chemistry and contamination; cw and pulsed chemical laser development including chemical kinetics, spectroscopy, optical resonators and beam pointing, atmospheric propagation, laser effects and countermeasures.

Chemistry and Physics Laboratory: Atmospheric chemical reactions, atmospheric optics, light scattering, state-specific chemical reactions and radiation transport in rocket plumes, applied laser spectroscopy, laser chemistry, battery electrochemistry, space vacuum and radiation effects on materials, lubrication and surface phenomena, thermionic emission, photosensitive materials and detectors, atomic frequency standards, and bioenvironmental research and monitoring.

Electronics Research Laboratory: Microelectronics, GaAs low-noise and power devices, semiconductor lasers, electromagnetic and optical propagation phenomena, quantum electronics, laser communications, lidar, and electro-optics; communication sciences, applied electronics, semiconductor crystal and device physics, radiometric imaging; millimeter-wave and microwave technology.

Information Sciences Research Office: Program verification, program translation, performance-sensitive system design, distributed architectures for spaceborne computers, fault-tolerant computer systems, artificial intelligence, and microelectronics applications.

Materials Sciences Laboratory: Development of new materials: metal matrix composites, polymers, and new forms of carbon; component failure analysis and reliability; fracture mechanics and stress corrosion; evaluation of materials in space environment; materials performance in space transportation systems; analysis of systems vulnerability and survivability in enemy-induced environments.

Space Sciences Laboratory: Atmospheric and ionospheric physics, radiation from the atmosphere, density and composition of the upper atmosphere, aurorae and airglow; magnetospheric physics, cosmic rays, generation and propagation of plasma waves in the magnetosphere; solar physics, infrared astronomy; the effects of nuclear explosions, magnetic storms, and solar activity on the earth's atmosphere, ionosphere, and magnetosphere; the effects of optical, electromagnetic, and particulate radiations in space on space systems.

END

FILMED

2-83

DTIC